



NOTICE: This material may be protected by copyright law. (Title 17 U.S. Code)

PII: S1089-3156(97)00016-0

PH: S1089-3156(97)00016-0

Provided by AFRL  
Technical Library

## The viscoelastic behaviour of networks

C. M. Roland\* and K. L. Ngai

Naval Research Laboratory, Washington, D.C. 20375-5342, USA

and D. J. Plazek

Department of Materials Science and Engineering, University of Pittsburgh, Pittsburgh, PA 15261, USA

(Received 23 September 1997; revised 29 October 1997)

Studies of relaxation in rubbery networks reveal a variety of behaviours. In experiments on networks with labelled junctions, whereby the motion of the crosslink site is specifically monitored, the segmental relaxation function broadens with increasing crosslink density, accompanied by a larger activation energy. Such results are well-described by theory. The more usual experiment simply measures bulk relaxation, without discriminating among different relaxing entities. For networks, crosslinking introduces a distribution of relaxation behaviours, related to the proximity of a moiety to the junctions. The resulting inhomogeneously broadened relaxation function is difficult to analyse; nevertheless, a heightened sensitivity to temperature (larger activation energy) is observed, from which inferences can be made regarding the shape of the segmental relaxation function. Crosslinking also influences the viscoelastic spectrum at times longer than that associated with local segmental relaxation, in a manner consistent with ideas based on constraint dynamics. © 1998 Elsevier Science Ltd. All rights reserved

(Keywords: networks; PTHF; viscoelasticity; polybutadiene; relaxation; epoxy resin)

### INTRODUCTION

Modern theories of rubber elasticity depart from the classical approaches in the account taken by the former of the effect of interactions among network chains<sup>1-7</sup>. Intermolecular constraints reduce the configurations available to the network, and thus can contribute to the elastic energy and its strain dependence. While the mechanical properties of networks can be described at least semi-quantitatively by elasticity theories<sup>3,8-10</sup>, only the equilibrium properties are usually addressed. However, experimental techniques such as quasielastic neutron scattering<sup>11,12</sup>, <sup>31</sup>P NMR<sup>13</sup>, and molecular dynamics simulations<sup>14</sup> probe the network dynamics, and thus stimulate interest in connecting the equilibrium and viscoelastic properties.

The coupling model of relaxation<sup>15</sup> considers the influence of constraints on the chain dynamics, providing insights into how dynamic constraints (which are chemical structure dependent) govern both the time and the temperature dependence of macroscopic relaxation properties<sup>16-21</sup>. More recently, the coupling model has been applied to the microscopic (sub-picosecond) dynamics<sup>22-31</sup>.

Obviously a connection must exist between the equilibrium mechanical properties of a network and its relaxation behaviour. Although little work has been done to systematically quantify these relationships, in a recent paper<sup>20</sup> we pointed out that various structural changes known to alleviate topological constraints on the network chains (e.g. lower crosslink functionality or density, the presence of diluent, orientation) can also be shown to reduce the degree of intermolecular cooperativity of the dynamics. Thus, relaxation models, such as the coupling model, potentially provide an interpretation of the elastic properties in terms of the constraint dynamics. Toward this end, this paper explores three relaxation phenomena—relaxation of junctions in an end-linked, unimodal network, local segmental relaxation in a randomly cross-linked elastomer, and the chain motions in epoxy resins.

### EFFECT OF CROSSLINKS ON JUNCTION MOTIONS

Shi *et al.*<sup>13</sup> carried out solid state <sup>31</sup>P NMR spin-lattice relaxation measurements on a series of polytetrahydrofuran networks of varying molecular weight between crosslinks. The NMR experiments

\*To whom correspondence should be addressed.

specifically measure the dynamics of the tris(4-isocyanatophenyl) thiophosphate junctions, since that is the sole location of phosphorus nuclei. The coupling model provides an interpretation of these results<sup>20</sup>. The relaxation conforms to the Kohlrausch function

$$C(t) = C_0 \exp - \left( \frac{t}{\tau_K} \right)^\beta \quad (1)$$

in which  $\tau_K$  is the relaxation time, and, according to the coupling model<sup>15-18</sup>, the stretch exponent  $\beta$  ( $0 < \beta < 1$ ) reflects the strength of the intermolecular constraints. A broader relaxation function, corresponding to a smaller  $\beta$ , implies stronger cooperativity. The best-fit values for the stretch exponent, listed in Table 1, reveal that an increasing crosslink density is associated with increasing intermolecular constraints (smaller  $\beta$ ) on the junction dynamics.

The results in Table 1 can be compared with the value for  $\beta$  reported previously<sup>18</sup>. From the dependence of the segmental relaxation time on scattering vector (momentum transfer), it was determined that for bulk, linear PTHF,  $\beta = 0.6 \pm 0.03$ . Such a large value indicates a modest degree of intermolecular coupling of the segmental relaxation, consistent with the very flexible ether linkage in the PTHF backbone. The NMR experiment only measures motion of the junctions, not the PTHF strands; nevertheless, the value in Table 1 is consistent with the earlier results<sup>18</sup>.

According to the coupling model, a relaxation function having the form of equation (1) is obtained only after the unbalanced torques and forces imposed by neighbouring segments have built up to an extent sufficient to slow down the relaxation. This requires some temperature-independent time period  $t_c$  (picoseconds), prior to which the relaxation is unconstrained, and governed by a non-cooperative relaxation time  $\tau_D$ . An expression for  $\tau_D$  is obtained from the continuity of the relaxation function at  $t_c$ <sup>15-18</sup>

$$\tau_D = \tau_K^\beta \times t_c^{1-\beta} \quad (2)$$

Table 1 Polytetrahydrofuran networks

$M_c$ (g mol <sup>-1</sup> )	650	1000	2000	2900
$\beta$	0.40	0.43	0.49	0.58

Table 2 Crosslinked polyvinylethylene

$M_c$ (g mol <sup>-1</sup> )	1100	1500	3800	Uncrosslinked
$\beta$	0.34	0.35	0.37	0.41

The (intermolecularly) non-cooperative dynamics is sometimes referred to as 'Debye relaxation'. If it has an Arrhenius temperature dependence, then from equation (2) the activation energy prevailing at short times,  $E_a$ , can be related to the activation energy,  $E_{a^*}$ , observed in the presence of intermolecular constraints by<sup>15-18</sup>

$$E_{a^*} = \frac{E_a}{\beta} \quad (3)$$

For non-Arrhenius behaviour, the relationship between the respective temperature dependencies of  $\tau_D$  and  $\tau_K$  becomes more complicated, but can still be quantitatively related (as shown below). Equations (2) and (3) have been used extensively to account for the well-known correlation between time and temperature dependencies of relaxation<sup>15-31</sup>.

We can apply this to the PTHF networks by noting that once the effects of intermolecular constraints have been removed (i.e. in going from  $\tau_K$  to  $\tau_D$  via equation (2)), the chemically-identical networks should exhibit very similar dynamics. To demonstrate this, we calculate the activation energy in the absence of constraints,  $E_a$  from the activation energy,  $E_{a^*}$ , determined experimentally from the change of  $\tau_K$  relaxation time with temperature. The results (Figure 1) show that  $E_a$  ( $= 6.3 \text{ kcal mol}^{-1}$ ) does not depend on crosslink density. Its magnitude reflects the bulky nature of the tris(4-isocyanatophenyl) thiophosphate junctions.

### EFFECT OF CROSSLINKS ON SEGMENTAL RELAXATION

In the NMR experiments described above, each relaxing species (i.e. the <sup>31</sup>P labelled junctions) had the same correlation function (i.e. homogeneous

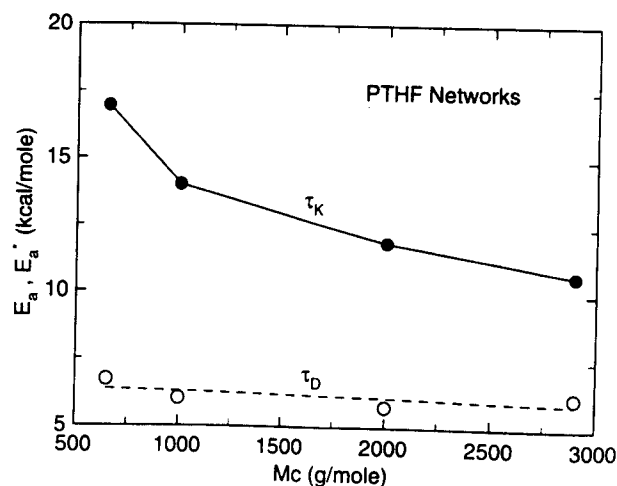
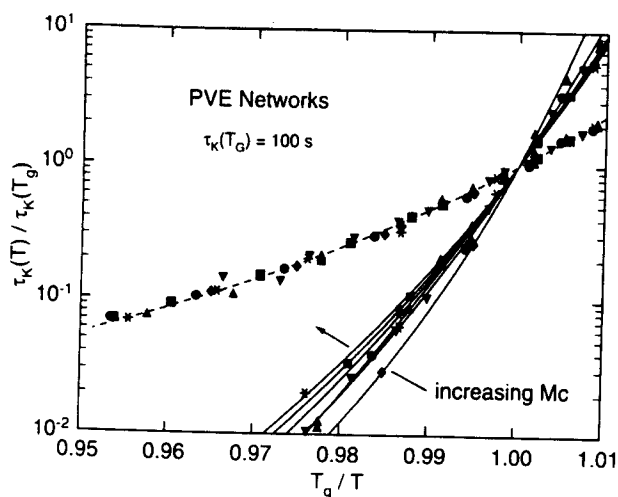


Figure 1 Activation energy for PTHF junctions as measured (●) and after subtraction (using equation (3)) of the effect of intermolecular constraints (○)

relaxation); consequently, the strength of the intermolecular constraints (i.e.  $\beta$ ) could be assessed by direct application of equation (1). For bulk spectroscopic techniques, networks exhibit a distribution of relaxation behaviours. Each can be described by equation (1), but the exact values of  $\tau_K$  and  $\beta$  may be spatially varying. Presumably, a chain segment more remote from a junction will experience relatively weaker coupling of its motion. For such inhomogeneous broadening, the magnitude of the intermolecular constraints on the dynamics can only be inferred from the change of the mean relaxation time (or peak frequency of the dispersion) with temperature.

Polyvinylethylene was reacted with varying concentrations of dicumyl peroxide to yield a series of networks with varying crosslink concentrations<sup>32</sup>. Free radicals formed at the vinyl carbons propagate with minimal termination to yield junctions of high functionality. The confluence of many network chains results in severe constraints in the vicinity of the crosslink sites. The degree of intermolecular cooperativity due to this crosslinking is expected to depend on a segment's proximity to the junctions.

Dielectric spectra were obtained at a series of temperatures slightly above the  $T_g$  of the PVE networks. In *Figure 2* are shown the mean relaxation times, defined from the maxima in the dielectric loss. The results are displayed in the fragility format developed by Angell<sup>33</sup>, wherein the temperature has been normalised by the glass transition temperature. Many experimental studies have shown that the fragility approach to analysing data is a valid basis for comparing temperature sensitivities of segmental relaxation<sup>16-18,21,34-40</sup>. Of course, when Arrhenius behaviour obtains (as in the pre-



**Figure 2** The segmental relaxation times, defined as the inverse of the maximum in the dielectric loss, for PVE networks (—) along with the superpositioned curves (---) obtained by raising  $\tau_K$  to the power of respective  $\beta$  for that network. The value of the stretch exponents deduced in this manner are listed in *Table 2*

vious NMR data on PTHF junctions),  $T_g$ -normalisation is not required to assess temperature dependencies.

Note that, in *Figure 2*, the weakest temperature dependence is that of linear (uncrosslinked) PVE. From fitting to equation (1),  $\beta = 0.41$  is obtained for its relaxation function. This value is consistent with an earlier study on PVE, employing both mechanical and dielectric spectroscopy, which found  $\beta$  to vary weakly with temperature<sup>41</sup>. The stretch exponent for PVE is relatively small, indicating that segmental relaxation of PVE is highly intermolecularly cooperative. This is a consequence of strong intermolecular coupling, due to steric constraints arising from the inflexible vinyl moiety present on alternate backbone carbons<sup>16</sup>.

The more highly crosslinked networks exhibit a stronger dependence of  $\tau_K$  on  $T_g$ -scaled temperature. Since this temperature sensitivity is quantitatively described by equations (2) and (3), the relaxation curves can be superimposed by scaling the  $\tau_K$  values for each network by their respective value of the exponent  $\beta$  (*Figure 2*). This allows mean values for the stretch exponent to be obtained, even though the measured relaxation functions are inhomogeneously broadened. The  $\beta$  values obtained by this procedure are listed in *Table 2*. Again we observe that increases in crosslink density effect more constrained segmental relaxation (i.e. smaller  $\beta$ ).

### EFFECT OF CROSSLINKS ON THE VISCOELASTIC SPECTRUM OF THE NETWORK STRANDS

While we have seen the manner in which higher crosslink densities enhance the constraints on the local segmental motions, in this section we discuss the effects of the junctions on the viscoelastic spectrum at longer times. Intuitively, junctions are expected to be more effective in constraining viscoelastic mechanisms having larger length scales (i.e. longer wavelengths). The largest effect should occur for the mode whose length scale corresponds to the molecular weight between crosslinks,  $M_c$ ; this mode is responsible for the equilibrium compliance of the network. We examine this by analysing creep compliance data on a series of cured epoxy resins<sup>42</sup>. The materials and some quantities relevant to the present work are listed in *Table 3*. More details can be found in earlier reports<sup>42,43</sup>.

To isolate the contribution due to local segmental motion, we subtract  $J_g$ , the glassy compliance, from the compliance function,  $J(t)$ . The difference,  $(J(t) - J_g)$ , is plotted in *Figure 3*. For compliance levels up to approximately  $4 \text{ GPa}^{-1}$ ,

Table 3 Cured epoxy resins

Designation <sup>a</sup>	$M_c$ (g mol <sup>-1</sup> ) <sup>b</sup>	$J_g$ (GPa <sup>-1</sup> )	$T_g$ (°C)	$T_{ref}$
Epon 828	420	1.82	204	205
Epon 1001	910	1.36	127	132
Epon 1004	1520	1.32	112	114
Epon 1007	2870	1.18	101	105

<sup>a</sup>Shell Chemical Company.

<sup>b</sup>Cured with stoichiometric amount of 4,4'-diamino diphenyl sulfone crosslinker.

$(J(t) - J_g)$  has a power law form, and is entirely due to local segmental motion. Note that this power law behaviour is a good approximation at short times to the stretched exponential form

$$J_\alpha(t) \equiv \Delta J_\alpha [1 - \exp(-t/\tau)^\beta] \quad (4)$$

found for the compliance contributed by the local segmental ( $\alpha$ -relaxation) retardation of several polymers<sup>44,45</sup>.  $\Delta J_\alpha$  is about 4 GPa<sup>-1</sup>. Values of  $(J(t) - J_g)$  higher than this reflect contributions from viscoelastic modes having length scales larger than that associated with local segmental motion. These mechanisms involve the 'sub-Rouse' modes<sup>21,46,47</sup> with shorter length scales (contributing at lower compliances) and the Rouse modes with longer lengthscale (contributing at higher compliances). For networks, the longest relevant length scale,  $L_c$ , of the viscoelastic modes is determined by  $M_c$ .

In Figure 3, the shift factor and the reference temperature,  $T_{ref}$ , for the most crosslinked resin, E828, are identical to the values used in Ref. 42. For the other three epoxies, additional horizontal shifts have been applied to superpose their power law regimes

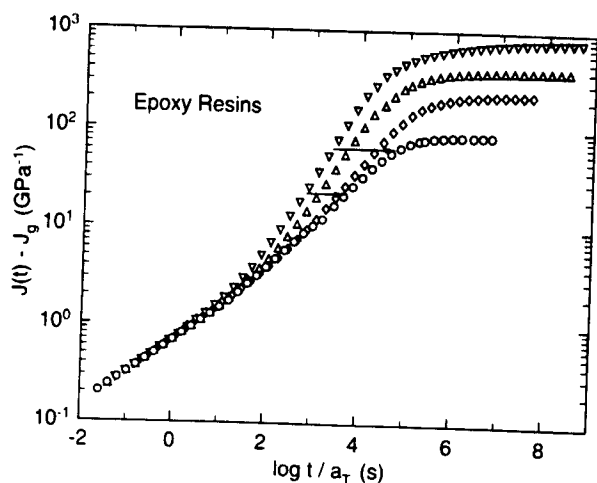


Figure 3 Creep curves after subtraction of the glassy compliance for Epon 828 (○), Epon 1001 (◇), Epon 1004 (△), and Epon 1007 (▽). The shift factor and reference temperature for E828 are identical to the values used in Ref. 42. For the other three samples, horizontal shifts of  $-0.73$ ,  $-1.18$ , and  $-1.5$  decades have been applied to superimpose the data in the short time regime associated with local segmental relaxation

with that of E828. Thus, at the respective reference temperatures (given in Table 3), all samples have the same local segmental retardation time.

The viscoelastic responses of the four epoxy resins in Figure 3 can now be compared. One obvious difference between them is the reduction of the equilibrium compliance of the network as the crosslink density is increased. This reduction is the obvious consequence of elimination of longer length scale viscoelastic modes as  $M_c$  decreases. More subtle is the displacements of the viscoelastic modes contributing at any compliance level toward longer times when the crosslink density is increased. The magnitude of the displacement is not uniform, but increases with the compliance (or equivalently the length scale of the viscoelastic mode), as illustrated by the two horizontal arrows in Figure 3. The result is the fanning out of the compliance curve for the epoxy with higher crosslink density from  $J(t) - J_g$  for the less-crosslinked epoxy. For longer times, the former levels off to its equilibrium compliance. Comparing the compliance curve of the tight network E828 with that of the loose network E1007, it can be seen that the maximum displacement of the former is large (about 2 decades). Thus, the longer length scale viscoelastic modes are more constrained by the crosslinks, and thus their relaxation is more retarded.

## CONCLUSION

In any densely packed system, the motions and configurations available to a polymer chain is governed by dynamical constraints originating from intermolecular interactions with neighboring chains and chain segments. An important objective of rubber elasticity theories is to provide a description of the consequences of these intermolecular constraints on the elastic properties. The coupling model addresses the manner in which the same constraints affect the relaxation properties. Common to both lines of inquiry is the conclusion that an increasing crosslink density magnifies the effect of intermolecular constraints.

## ACKNOWLEDGEMENT

This work was supported by the Office of Naval Research.

## REFERENCES

1. Eichinger, B. E., *Ann. Rev. Phys. Chem.*, 1983, **34**, 359.
2. Flory, P. J., *J. Chem. Phys.*, 1977, **66**, 5720.
3. Flory, P. J. and Erman, B., *Macromolecules*, 1982, **15**, 800.

4. Erman, B. and Monnerie, L., *Macromolecules* 1992, **25**, 4456.
5. Vilgis, T. A. and Erman, B., *Macromolecules*, 1993, **26**, 6657.
6. Kloczkowski, A., Mark, J. E. and Erman, B., *Macromolecules*, 1995, **28**, 5089.
7. Erman, B. and Mark, J. E., *Structures and Properties of Rubber-like Networks*. Oxford University Press, New York, 1997.
8. Pak, H. and Flory, P. J., *J. Polym. Sci. Polym. Phys. Ed.*, 1979, **17**, 1845.
9. Fontaine, F., Noel, C., Monnerie, L. and Erman, B., *Macromolecules*, 1989, **22**, 3352.
10. Mott, P. H. and Roland, C. M., *Macromolecules*, 1996, **29**, 6941.
11. Higgins, J. S., Ma, K. and Hall, R. H., *J. Phys. C*, 1981, **14**, 4995.
12. Oeser, R., Ewen, B., Richter, D. and Farago, B., *Phys. Rev. Lett.*, 1988, **60**, 1041.
13. Shi, J.-F., Dickinson, L. C., MacKnight, W. J. and Chien, J. C. W., *Macromolecules*, 1993, **26**, 5908.
14. Duering, E. R., Kremer, K. and Grest, G. S. (a) *Phys. Rev. Lett.*, 1991, **67**, 3531; (b) *Macromolecules*, 1993, **26**, 3241.
15. (a) Ngai, K. L., *Comments Solid State Phys.*, 1979, **9**, 127; (b) Tsang, K.-Y. and Ngai, K. L., *Phys. Rev. E*, 1996, **54**, R3067; (c) Ngai, K. L. in *Disorder Effects on Relaxational Processes*, eds R. Richert and A. Blumen. Springer, Berlin, 1994, p. 89.
16. Roland, C. M. and Ngai, K. L., (a) *Macromolecules*, 1991, **24**, 5315; (b) *Macromolecules*, 1992, **25**, 1844.
17. Roland, C. M. and Ngai, K. L., *Macromolecules*, 1992, **25**, 5765.
18. Ngai, K. L. and Roland, C. M., *Macromolecules*, 1993, **26**, 6824.
19. Ngai, K. L., Roland, C. M. and Yee, A. F., *Rub. Chem. Tech.*, 1993, **66**, 817.
20. Ngai, K. L. and Roland, C. M., *Macromolecules*, 1994, **27**, 2454.
21. Ngai, K. L. and Plazek, D. J., *Rub. Chem. Tech.*, 1995, **68**, 376.
22. Roland, C. M. and Ngai, K. L., *J. Non-Crystalline Solids*, 1997, **212**, 74.
23. Roland, C. M. and Ngai, K. L., *Macromolecules*, 1996, **29**, 5747.
24. Roland, C. M., Santangelo, P. G., Baram, Z. and Runt, J., *J. Macromolecules*, 1994, **27**, 5382.
25. Ngai, K. L. and Roland, C. M., *J. Phys. Chem.*, 1997, **101**, 4437.
26. Roland, C. M. and Ngai, K. L., *J. Chem. Phys.*, 1997, **106**, 1187.
27. Ngai, K. L. and Roland, C. M., *Phys. Rev. E*, 1996, **54**, 6969.
28. Ngai, K. L. and Roland, C. M., *Phys. Rev. E*, 1997, **55**, 2069.
29. Roland, C. M., Ngai, K. L. and Lewis, L. J., *J. Chem. Phys.*, 1995, **103**, 4632.
30. Roland, C. M. and Ngai, K. L., *J. Chem. Phys.*, 1996, **104**, 2967.
31. Roland, C. M. and Ngai, K. L., *J. Chem. Phys.*, 1995, **103**, 1152.
32. Roland, C. M., *Macromolecules*, 1994, **27**, 4242.
33. Angell, C. A., *J. Non-Cryst. Solids*, 1991, **131-133**, 13.
34. Böhmer, R., Ngai, K. L., Angell, C. A. and Plazek, D. J., *Chem. Phys.*, 1991, **94**, 3018.
35. Roland, C. M. and Ngai, K. L., *Macromolecules*, 1991, **24**, 2261.
36. Roland, C. M. and Ngai, K. L., *Macromolecules*, 1992, **25**, 363.
37. Roland, C. M., *Macromolecules*, 1992, **25**, 7031.
38. Ngai, K. L. and Roland, C. M., *Macromolecules*, 1993, **26**, 2688.
39. Roland, C. M., Santangelo, P. G., Ngai, K. L. and Meier, G., *Macromolecules*, 1993, **26**, 6164.
40. Santangelo, P. G., Ngai, K. L. and Roland, C. M., *Macromolecules*, 1994, **27**, 3859.
41. Colmenero, J., Alegria, A., Santangelo, P. G., Ngai, K. L. and Roland, C. M., *Macromolecules*, 1994, **27**, 407.
42. Plazek, D. J. and Choy, I.-C., *J. Polym. Sci.: Part B: Polym. Phys.*, 1989, **27**, 307.
43. LeMay, J. D., Swetlin, B. J. and Kelley, F. N., *ACS Symp. Series*, 1984, **243**, 177.
44. Plazek, D. J., Bero, C. A., Neumeister, S., Floudas, S., Fytas, G. and Ngai, K. L., *Colloid Polym. Sci.*, 1994, **272**, 1430.
45. Ngai, K. L., Plazek, D. J. and Echeverria, I., *Macromolecules*, 1996, **29**, 1931.
46. Santangelo, P. G., Ngai, K. L. and Roland, C. M., *Macromolecules*, 1993, **26**, 2682.
47. Plazek, D. J., Chay, I.-C., Ngai, K. L. and Roland, C. M., *Macromolecules*, 1995, **28**, 6432.